

Article

Synthesis and Biological Activity of Novel α -Conotoxins Derived from Endemic Polynesian Cone Snails

Yazid Mohamed Souf ¹, Gonxhe Lokaj ², Veeresh Kuruva ³, Yakop Saed ³, Delphine Raviglione ¹, Ashraf Brik ³, Annette Nicke ², Nicolas Inguibert ^{1,*} and Sébastien Dutertre ^{4,*}

¹ CRIOBE, UAR CNRS-EPHE-UPVD 3278, Université de Perpignan Via Domitia, 58 Avenue Paul Alduy, 66860 Perpignan, France; yazid.souf@univ-perp.fr (Y.M.S.); delphine.raviglione@univ-perp.fr (D.R.)

² Faculty of Medicine, Walther Straub Institute of Pharmacology and Toxicology, Ludwig Maximilian University of Munich, Nußbaumstraße 26, 80336 Munich, Germany; g.lokaj@lmu.de (G.L.); annette.nicke@lrz.uni-muenchen.de (A.N.)

³ Schulich Faculty of Chemistry, Technion-Israel Institute of Technology, Haifa 3200008, Israel; veeresh1590@gmail.com (V.K.); vkyakop.saed@campus.technion.ac.il (Y.S.); abrik@technion.ac.il (A.B.)

⁴ IBMM, Université Montpellier, CNRS, ENSCM, 34093 Montpellier, France

* Correspondence: nicolas.inguibert@univ-perp.fr (N.I.); sebastien.dutertre@umontpellier.fr (S.D.)

Abstract: α -Conotoxins are well-known probes for the characterization of the various subtypes of nicotinic acetylcholine receptors (nAChRs). Identifying new α -conotoxins with different pharmacological profiles can provide further insights into the physiological or pathological roles of the numerous nAChR isoforms found at the neuromuscular junction, the central and peripheral nervous systems, and other cells such as immune cells. This study focuses on the synthesis and characterization of two novel α -conotoxins obtained from two species endemic to the Marquesas Islands, namely *Conus gauguini* and *Conus adamsonii*. Both species prey on fish, and their venom is considered a rich source of bioactive peptides that can target a wide range of pharmacological receptors in vertebrates. Here, we demonstrate the versatile use of a one-pot disulfide bond synthesis to achieve the α -conotoxin fold [Cys 1-3; 2-4] for GaIA and AdIA, using the 2-nitrobenzyl (NBzl) protecting group of cysteines for effective regioselective oxidation. The potency and selectivity of GaIA and AdIA against rat nicotinic acetylcholine receptors were investigated electrophysiologically and revealed potent inhibitory activities. GaIA was most active at the muscle nAChR (IC₅₀ = 38 nM), whereas AdIA was most potent at the neuronal $\alpha 6/3 \beta 2\beta 3$ subtype (IC₅₀ = 177 nM). Overall, this study contributes to a better understanding of the structure–activity relationships of α -conotoxins, which may help in the design of more selective tools.

Keywords: conotoxin; peptide synthesis; two-electrode voltage clamp; nicotinic acetylcholine receptors



Citation: Souf, Y.M.; Lokaj, G.; Kuruva, V.; Saed, Y.; Raviglione, D.; Brik, A.; Nicke, A.; Inguibert, N.; Dutertre, S. Synthesis and Biological Activity of Novel α -Conotoxins Derived from Endemic Polynesian Cone Snails. *Mar. Drugs* **2023**, *21*, 356. <https://doi.org/10.3390/md21060356>

Academic Editor: Richard J. Lewis

Received: 17 May 2023

Revised: 6 June 2023

Accepted: 7 June 2023

Published: 9 June 2023



Copyright: © 2023 by the authors. Licensee MDPI, Basel, Switzerland. This article is an open access article distributed under the terms and conditions of the Creative Commons Attribution (CC BY) license (<https://creativecommons.org/licenses/by/4.0/>).

1. Introduction

Polynesia is an archipelago made up of over 100 islands spread over an area of 4 million km². It is further divided into five archipelagos: the Society Islands, the Marquesas Islands, the Tuamotu Islands, the Gambier Islands, and the Austral Islands. Due to their geographical isolation, the islands of Polynesia have developed unique flora and fauna, with many endemic species found nowhere else in the world. Endemic cone snails of Polynesia are remarkable examples of this biodiversity, as these species are rare and unique to this region. These snails are characterized by their unique shells, which are often brightly colored and beautifully patterned. Among the most iconic are *Conus gauguini* (named after French painter Paul Gauguin) and *Conus adamsonii*, which are favorites among shell collectors.

Nearly 1000 different species of these venomous marine mollusks have been described, and more than 20% are located in Polynesia [1]. They produce potent venom made up of hundreds of small peptides called conotoxins. These peptides can target a wide range

of receptors, ion channels, and transporters. The cysteine framework, gene superfamily, and their pharmacological targets are used to classify the conopeptides [2]. Ziconotide, a synthetic version of the ω -conotoxin MVIIA, was isolated from *Conus magus* venom and approved by the FDA in 2004 for the treatment of chronic pain. It constitutes one of the very few drugs derived from marine natural compounds [3]. While ω -conotoxins block N-type calcium channels, the α -conotoxins target the nicotinic acetylcholine receptors (nAChRs), which are ion channels of primary physiological importance [4–6]. Indeed, nAChRs are widely distributed in the central nervous system (CNS) and the periphery, with several subtypes known to be involved in pain sensation, attention, learning, and memory. Thus, nAChRs are attractive pharmacological targets with potential applications in the treatment of pain, memory disorders, or Parkinson's disease. To date, 16 homologous nAChR subunits have been identified in mammals (α 1–7, α 9, α 10, β 1–4, δ , and ϵ/γ), which can assemble in numerous combinations to form pentameric complexes of different nAChR subtypes [7–9]. The specific functions of each subtype are not fully understood, and α -conotoxins are among the most specific molecules that are capable of helping decipher their function [6,7,10–12].

In this work, we focused on the synthesis and functional characterization of two novel α -conotoxins, GaIA and AdIA, from the piscivorous cones *C. gauguini* and *C. adamsonii*, respectively. Both species are endemic to the Marquesas Islands. We applied a novel one-pot synthesis that leads directly to the native peptide. This was achieved by using the 2-nitrobenzyl (NBzl) protecting group in conjunction with the triphenylmethyl (Trt) group to ensure successful regioselective folding. This strategy was compared with the more commonly used oxidative folding strategies, which are based on thermodynamically driven folding of fully unprotected precursors or the use of the acetamidomethyl (Acm) and Trt protecting groups. Biological characterization using the two-electrode voltage clamp method revealed potent inhibitory activities at different nAChRs.

2. Results

2.1. α -Conotoxin Sequences

Two α -conotoxins, GaIA and AdIA, were retrieved from our in-house transcriptomic data on the piscivorous cones *C. gauguini* and *C. adamsonii* (to be published elsewhere), respectively. These conotoxins contain four cysteines and a predicted amidated C-terminus (Table 1). These conopeptides belong to different Cys loop spacing frameworks with varying m/n-loop sizes (m and n designate the number of non-cysteine residues between the conserved cysteine residues) identified in α -conotoxins, including α -3/5, α -3/7, α -4/5, α -4/7, and α -4/4. Interestingly, these frameworks appear to confer some subtype selectivity [11]. GaIA belongs to the α -3/5 sub-family, and AdIA belongs to the α -4/4 sub-family [13–15]. Since most characterized α -conotoxins belong to the 4/7 family and only comparably few 3/5 and 4/4 peptides have been synthesized and investigated before, we aimed to study their potency on specific nicotinic acetylcholine receptor subtypes (nAChRs). The 3/5 framework of GaIA generally affects muscle-type nAChR receptors [16–18], while the 4/4 framework of AdIA is of particular interest because it has been found to target both muscle-type and neuronal nAChR receptor subtypes [11]. AdIA appears very similar to BuIA, which targets several neuronal subtypes [19] and differs by only one residue from AdIA (BuIA has a tyrosine residue instead of a histidine residue in position 13). GaIA is most closely related to α -MI and α -GI, and all three have the following sequence in common: GXCCXPACGXXYXC (Table 1). A comparison of the potencies and sequences of these variants has the potential to reveal the molecular basis for the design of compounds with better selectivity for nAChR subtypes. From a chemical perspective, the presence of two neighboring proline residues in the sequence of AdIA represents a synthetic challenge due to potential folding difficulties. Furthermore, it might influence the overall structure and selectivity of the peptide, which makes the synthesis and study of these conopeptides a valuable contribution to the fields of both peptide synthesis and drug discovery.

Table 1. Sequence alignment between α -conotoxin identified from Polynesian cone snails and previously reported α -conotoxins.

Framework Loop	Conotoxin	Title 3	Species
3/5	GaIA	GRCCHPACGRKYNC *	<i>Conus gauquini</i>
	MI	GRCCHPACGKNYSC *	<i>Conus magus</i>
	GI	ECCNPACGRHYSC *	<i>Conus geographus</i>
4/4	AdIA	GCCSTPPCAVLHC *	<i>Conus adamsonii</i>
	BuIA	GCCSTPPCAVLYC *	<i>Conus bullatus</i>
4/4	LvIC	DCCANPVCNGKHCQ	<i>Conus lividus</i>
	[Δ Q14]LvIC	DCCANPVCNGKHC *	
	[D1G, Δ Q14]LvIC	GCCANPVCNGKHC *	

* C-terminally amidated.

2.2. Synthesis of Conotoxins

In order to compare the use of the Trt/Acm or Trt/NBzl pairs of cysteine protective groups for the preparation of α -conotoxins, we achieved the synthesis of the main precursors bearing a Trt at Cys II–IV and an Acm or NBzl at Cys I–III by Fmoc solid-phase peptide synthesis (SPPS) with an automated peptide synthesizer. The amino acid sequence of each precursor peptide is given in Supplementary Materials (Table S1). The initial linear peptides with a free thiol at positions II and IV were obtained after the cleavage of the peptide from the resin with similar yields and purity (Figures 1a and 2a). Trt groups were removed during the cleavage step, while the Nbzl and Acm protective groups are resistant to the cleavage conditions described in experimental procedures. The first disulfide bridge was formed by treatment with disulfiram (DSF). While the high-performance liquid chromatography (HPLC) profile for the pair Trt/NBzl appears to be devoid of any impurity (Figures 1b and 2b), the one obtained for GaIA with the Trt/Acm pair contains additional peaks (Figure S1B). The second disulfide bonds were then formed by UV irradiation using NBzl as protecting groups or after successive treatment with PdCl₂, DTC, and DSF for the Acm (Figures S1B and S2B). All the protocols are detailed in the experimental procedures [20,21].

The GaIA sequence does not contain any amino acids that may constrain its three-dimensional structure. Therefore, both approaches led to the desired isomer with ease, as shown in Figures 1 and S1. On the other hand, the AdIA sequence is unusual due to the presence of a Pro–Pro sequence, which allows for two different spatial configurations (Proline *cis* or *trans*). This particularity is interesting in terms of folding, and the *cis/trans* conformational dynamic equilibrium can be observed through the broadening of the peak during HPLC analysis at 24 °C, as depicted in Figure 2c (rt: 27.5 to 28.5 min). At lower temperatures (15.0 °C), we observed mostly a single conformer. The change in the *cis/trans* conformational equilibrium with temperature is shown in Supplementary Materials (Figure S3). Similar HPLC peak broadening was also observed in the previously reported Pro–Pro containing the conotoxin BuIA [22].

Fully oxidized peptides were purified by RP-HPLC, and the molecular weights were confirmed using high-resolution mass spectrometry (HRMS) (Figures S4 and S5). Mass spectral analyses of fully oxidized GaIA showed a mass of 1561.640 Da after deconvolution, which is consistent with the expected theoretical mass (1561.6271 Da). Similarly, AdIA showed a mass of 1284.4890 Da after deconvolution, which matches the expected theoretical mass (1284.4871 Da). Overall, the final yields for the non-directed folding synthesis approach were approximately 7% for GaIA (for which only one isomer was obtained and hence a simpler purification step) and only 2–3% for the globular isomer of AdIA. In contrast, the “one-pot” method produced almost twice as high yields (13% for GaIA and 10% for AdIA via NBzl’s approaches).

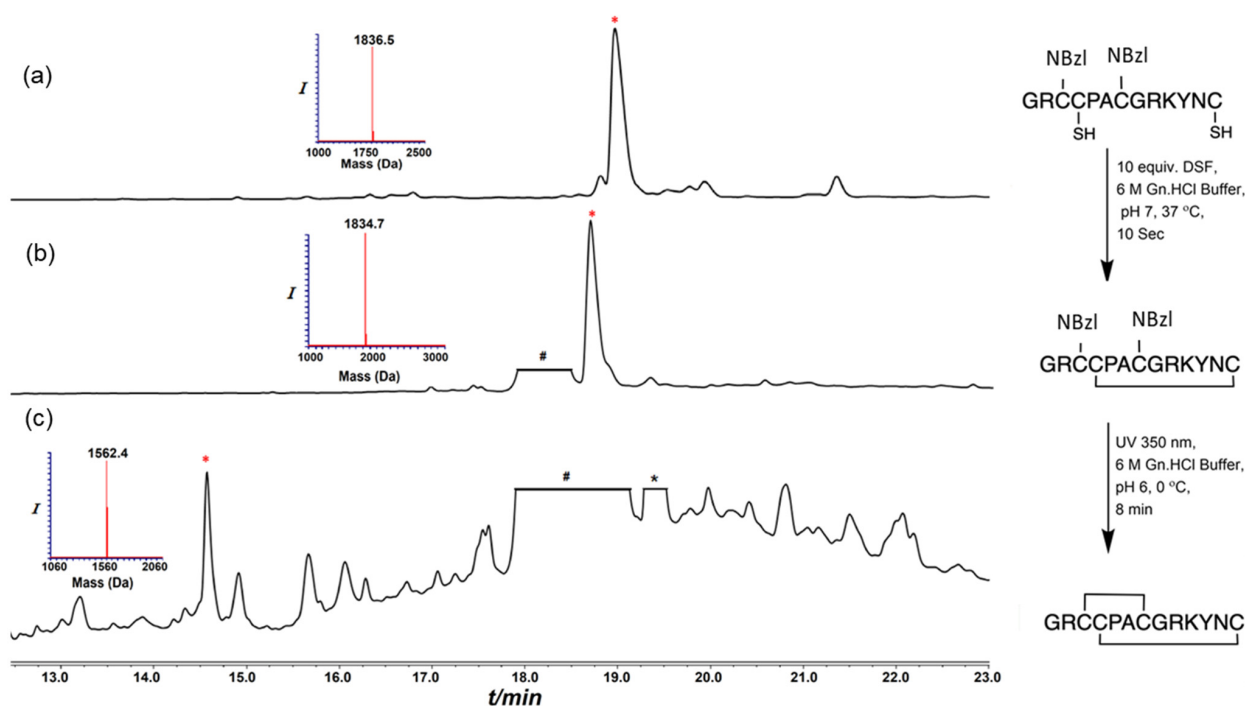


Figure 1. HPLC–MS analyses, GaIA synthesis via NBzl protecting groups; (a) the main peak observed corresponds to linear GaIA modified with NBzl at Cys I–III; (b) reaction after treating equiv. DSE, GaIA containing one disulfide bond; (c) reaction after UV radiation at 350 nm: conotoxin GaIA bearing two disulfide bonds. * non-peptide mass; * (red) desire product; and # non-peptide mass corresponding to DSE.

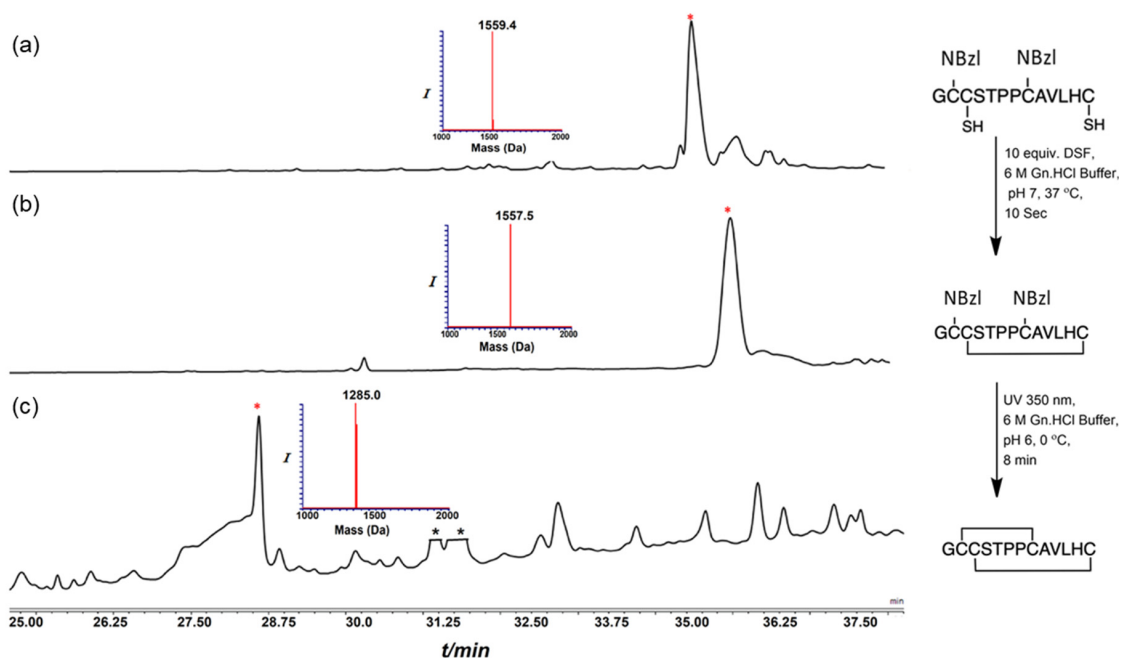


Figure 2. HPLC–MS analyses, AdIA synthesis via NBzl protecting groups; (a) the main peak observed corresponds to AdIA modified with NBzl at Cys I–III; (b) reaction after treating equiv. DSE, AdIA containing one disulfide bond; (c) reaction after UV radiation at 350 nm: conotoxin AdIA bearing two disulfide bonds. * non-peptide mass; * (red) desire product.

2.3. Functional Characterization

The inhibitory potency of AdIA and GaIA was investigated by two-electrode voltage clamp analysis on the following rat nAChR subtypes expressed in *Xenopus laevis* oocytes (Figure 3): the embryonic muscle-type nAChR ($\alpha 1\beta 1\gamma\delta$), the homomeric neuronal $\alpha 7$ nAChR, the heteromeric $\alpha 2\beta 2$, $\alpha 3\beta 2$, $\alpha 3\beta 4$, $\alpha 4\beta 2$, $\alpha 4\beta 4$ subtypes, and the $\alpha 6/\alpha 3\beta 4$ and $\alpha 6/\alpha 3\beta 2\beta 3$ combinations, in which an $\alpha 6/\alpha 3$ chimera was used to reconstitute the respective $\alpha 6$ binding sites since $\alpha 6$ has been difficult to express [23] (Table 1). AdIA was most potent at the $\alpha 6/\alpha 3\beta 2\beta 3$ nAChR with a half maximal inhibitory concentration (IC_{50}) of 177.3 nM but also inhibited $\alpha 3\beta 2$ ($IC_{50} = 1375$ nM) with lower potency. No inhibition greater than 50% was observed for any of the other nAChRs at concentrations up to 10 μ M.

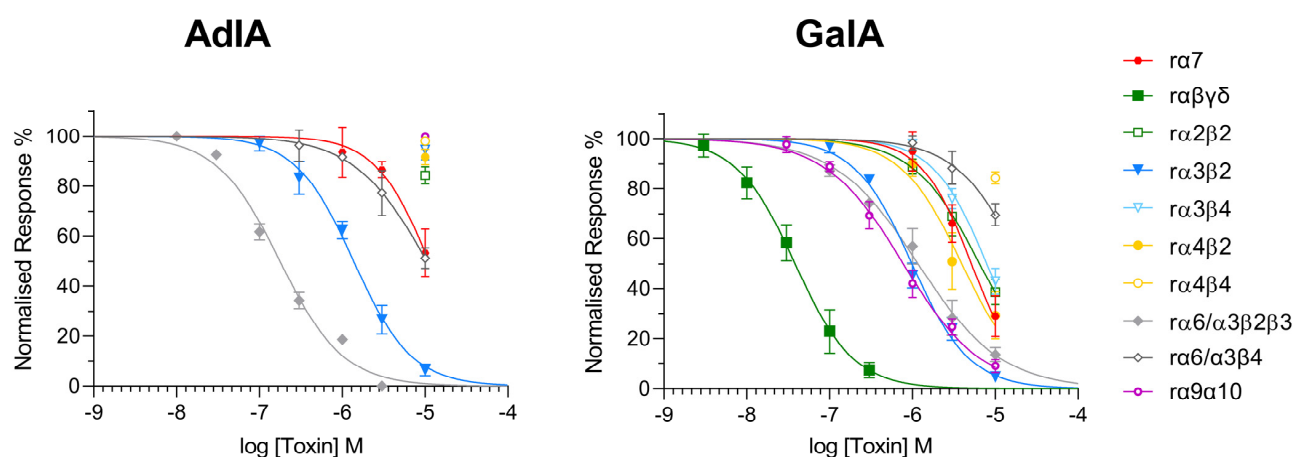


Figure 3. Dose–inhibition curves of AdIA (left) and GaIA (right) for the indicated rat nAChR subtypes expressed in *Xenopus laevis* oocytes. Two-electrode voltage clamp experiments were performed at -70 mV. Responses to 2-s pulses of 100 μ M ACh were recorded after a 3-min preincubation with the indicated peptides. Each point represents the mean of at least three to four measurements with oocytes from at least two frogs.

GaIA showed low nanomolar potency ($IC_{50} = 38.37$ nM) at the muscle-type nicotinic receptor $\alpha 1\beta 1\gamma\delta$. However, it also inhibited the neuronal $\alpha 3\beta 2$ nAChRs and the closely related $\alpha 6/\alpha 3\beta 2\beta 3$ nAChR with about 25-fold less potency ($IC_{50} = 988.9$ nM and $IC_{50} = 1170$ nM, respectively). IC_{50} values at the other neuronal nicotinic acetylcholine receptors were above 1 μ M ($\alpha 4\beta 2$: $IC_{50} = 3931$ nM, $\alpha 7$: $IC_{50} = 5158$ nM), $\alpha 2\beta 2$: $IC_{50} = 6474$ nM, $\alpha 3\beta 4$: $IC_{50} = 7912$ nM, $\alpha 6/\alpha 3\beta 4$: $IC_{50} = 18,160$ nM, and $\alpha 4\beta 4$: $IC_{50} = 49,430$ nM) (Table 2).

Table 2. IC_{50} values (in nM) of the conotoxins AdIA and GaIA on the indicated nAChR subtypes.

nAChRs (Rat)	AdIA		GaIA		BuIA	
	Toxin (IC_{50}) nM	Hill Slope	Toxin (IC_{50}) nM	Hill Slope	Toxin (IC_{50}) nM	Hill Slope
$\alpha 7$	>10.000	N.D.	5158 (4048 to 6680)	-1.45 (-1.60 to -1.02)	272 (243 to 304)	-1.21 (-1.10 to -1.32)
$\alpha\beta\gamma\delta$	N.D.	N.D.	38.37 (32.44 to 45.40)	-1.23 (-1.49 to -1.03)	N.D.	N.D.
$\alpha 2\beta 2$	>10.000	N.D.	6474 (5296 to 8167)	-1.09 (-1.39 to -0.83)	800 (567 to 1130)	-0.850 (-0.591 to -1.11)
$\alpha 3\beta 2$	1375 (1201 to 1574)	-1.24 (-1.46 to -1.07)	988.9 (867.9 to 1128)	-1.25 (-1.45 to -1.09)	5.72 (4.57 to 7.16)	-1.48 (-1.04 to -1.92)
$\alpha 3\beta 4$	>10.000	N.D.	7912 (6638 to 9680)	-1.37 (-1.76 to -1.06)	27.7 (22.3 to 34.5)	-1.52 (-1.01 to -2.04)
$\alpha 4\beta 2$	>10.000	N.D.	3931 (2578 to 6466)	-1.28 (-1.86 to -0.71)	>10.000	N.D.
$\alpha 4\beta 4$	>10.000	N.D.	>10.000	N.D.	69.9 (47.9 to 102)	-1.15 (-0.738 to -1.57)

Table 2. Cont.

nAChRs (Rat)	AdIA		GaIA		BuIA	
	Toxin (IC ₅₀) nM	Hill Slope	Toxin (IC ₅₀) nM	Hill Slope	Toxin (IC ₅₀) nM	Hill Slope
$\alpha 6 / \alpha 3 \beta 2 \beta 3$	177.3 (153.3 to 205.4)	−1.14 (−1.32 to −0.99)	1170 (996.9 to 1376)	−0.87 (−1.0 to −0.76)	0.26 (0.207 to −0.320)	−0.963 (−0.815 to −1.11)
$\alpha 6 / \alpha 3 \beta 4$	>10.000	N.D.	>10.000	N.D.	1.54 (1.32 to −1.78)	−1.40 (−1.12 to −1.68)
$\alpha 9 \alpha 10$	>10.000	N.D.	777.2 (679.8 to 889.3)	−0.93 (−1.04 to −0.83)	N.D.	N.D.
References	This work	This work	This work	This work	[13]	

95% confidence interval (CI) values are shown in parentheses. N.D. = not determined.

3. Discussion

α -Conotoxins are venom components that are used by cone snails to aid in prey capture and defense against predators [24]. Due to their action on nAChRs, they also represent useful pharmacological probes to decipher their physiological roles and reveal the therapeutic potential of nAChR selective modulators. Indeed, nAChRs are ion channels involved in the modulation of neurotransmission in the central and peripheral nervous systems. The search for the most appropriate ligand for a given nAChR subtype has greatly benefited from the α -conotoxin chemiodiversity inherited from the evolution of *Conus* species in different environments [25,26]. Additionally, advancements in chemical synthesis techniques and pharmacological characterization [16,27] have further facilitated the exploration of these compounds for their pharmacological properties. In this project, we are taking advantage of two endemic species from French Polynesia, *Conus gauquini* and *Conus adamsonii*, which produce the α -conotoxin GaIA and AdIA, respectively. These two conotoxins have not yet been synthesized or isolated from crude venom, but they could be useful in furthering our knowledge of nAChRs. Similar to most α -conotoxins, GaIA and AdIA possess four cysteine residues (that are predicted to form two disulfide bridges), which gives rise to three possible conformers, but the Cys I–III and Cys II–IV connectivity allows for a globular fold, which is the one found in these naturally occurring peptides [28,29].

The synthesis of these peptides can be achieved using two concurrent approaches: one based on the oxidative folding of a linear precursor with all thiols free, and the other on the regioselective and stepwise formation of individual disulfide bridges. While the first approach is attractive because only two disulfide bridges need to be formed, the correct folding conditions need to be optimized to favor the globular isomer [28,29]. In addition, purification processes are time-consuming as the compound is usually diluted in large volumes to avoid the formation of interchain bridges. In this case, the random formation of disulfide bridges is thermodynamically driven but is also a sequence-dependent process in which the more stable isomer is generally formed. Therefore, work was initiated by Gyanda et al. [21] to address this issue, and 30 different oxidation conditions were tested on various types of α -conotoxins to determine the best conditions leading to the formation of the globular isomer. Considering this study, we applied a buffer system of 0.1 M NH_4HCO_3 pH 8 with reduced and oxidized glutathione (GSH 100 eq/GSSG 10 eq), suitable for the $\alpha 3 / 5$ GaIA linear precursor. Additionally, we obtained a folded peptide in 48–72 h (Figure S7). For $\alpha 4 / 4$ conopeptides such as AdIA, very few experimental conditions have led to the formation of the globular isomer [28]. In most cases, oxidative folding has led to the formation of the ribbon isomer (Cys I–IV, Cys II–III). Nevertheless, the use of a 50/50 mixture of 0.1 M tris(hydroxymethyl)aminomethane (Tris.HCl)/isopropanol (IPA) (50/50), pH 8, with GSH/GSSG (100/10) at room temperature led to the correctly folded isomer for AdIA. This correctly folded isomer accounted for 70% of the different isomers observed (as depicted in Supplementary Materials, Figure S8). The use of an organic solvent, especially for peptides with hydrophobic side chains such as AdIA, enables the prevention of peptide self-aggregation, thereby promoting proper folding. To ascertain whether the Cys I–III and Cys II–IV linkages were formed using the previously described strategy based on random

oxidative folding, we synthesized the ribbon isomer of AdIA regioselectively. Furthermore, we performed a comparison with the peptides obtained through a regioselective approach and oxidative folding (Figures S6 and S9).

In recent years, several regioselective strategies have been developed, whether in solution or on solid support [30–32]. The synthesis of disulfide bond peptides typically involves the use of more than two protective groups for cysteines and often requires several synthesis steps with purification stages that can negatively impact final yields. However, a new method has been recently introduced that offers a one-pot regioselective approach [21]. For both approaches, using either NbzI or AcM as protective groups, the folded peptides are obtained in less than 30 min. It is worth noting that the use of DSF in this one-pot method provides an advantage, allowing for the rapid formation of disulfide bonds in less than ten seconds. Controlling the oxidation process requires maintaining the appropriate pH level. If the pH is below 5, the crude peptide will only partially form the S– bond. Conversely, if the pH exceeds 7.5, disulfide bridge opening and bond reshuffling to form regioisomers can be observed, as we can see with the presence of ribbon isomers in Figure S9.

Additionally, achieving proper folding for certain sequences, such as AdIA, can be challenging due to the presence of a Pro–Pro motif that creates a spatial conformation unfavorable for globular isomers. However, conducting the reaction at 37 °C can assist in such cases by causing further denaturation of the peptide chain, which ultimately facilitates the completion of the final bridge. In addition to the versatility of this method, there is also the fact that it improves the yield of synthesis compared to oxidative folding by nearly two folds.

In both cases, the yield of non-directed folding synthesis was approximately twice as low compared to the “one-pot” method via NBzI’s approaches (7% for GaIA and 2–3% for AdIA vs. 13% and 10%, respectively). Moreover, in challenging cases such as AdIA, the presence of the major isomer facilitates purification. Concerning the two “one-pot” strategies, the use of NBzI is more convenient as it requires less time and manipulation than the use of AcM, specifically for deprotection. In general, for most α -conotoxins, the synthetic strategy is based on the use of the Trt/AcM pairs. Often, this involves the use of I₂ to deprotect the AcM group. It has been established that the employment of this particular reagent may give rise to back-alkylation, or excessive oxidation of sulfonic acid, which can cause further adverse effects [33].

To date, only a few α -4/4 subfamily α -conotoxins have been characterized, including BuIA and LvIC [13,14]. BuIA showed low to medium nanomolar potency at α 6/ α 3 β 2 β 3 (IC₅₀ = 0.26 nM) and α 6/ α 3 β 4 (IC₅₀ = 1.54 nM) as well as α 3 β 2 (IC₅₀ = 5.72 nM) and α 3 β 4 (IC₅₀ 27.7, Table 1). Selectivity for α 6/ α 3 β 4 over α 3 β 4 (IC₅₀ = 1200 nM) and all other subtypes was obtained in the analog [T5A,P60]BuIA (IC₅₀ = 58.1 nM) [34].

LvIC inhibited only α 6/ α 3 β 4 with a micromolar potency (IC₅₀ = 3.3 μ M) but hardly inhibited other subtypes at concentrations up to 10 μ M. Remarkably, both potency and specificity for the α 6/ α 3 β 4 nAChR were significantly improved in [D1G, Δ Q14]LvIC (IC₅₀ = 19 nM) [14]. Interestingly, the closely related AdIA (= [Y13H] BuIA) shows selectivity for the α 6 β 2 interface with an IC₅₀ value of 177.3 nM at the α 6/ α 3 β 2 β 3 combination (α 3 is considered a structural subunit that does not form a binding site). In contrast, it shows potency that is at least 8-fold lower at α 3 β 2 (IC₅₀ = 1375 nM) and micromolar potency (>10 μ M) at all other subtypes. This makes it the first 4/4 framework α -conotoxin selective for the α 6 β 2 interface.

GaIA belongs to the α -3/5 subfamily and is closely related to α -MI and α -GI. These α -conotoxins have been widely studied for their high selectivity towards different interfaces of the muscle type and Torpedo nicotinic receptors. Likewise, the newly synthesized peptide GaIA shows nanomolar potency at the muscle-type α 1 β 1 γ δ nAChR with a similar IC₅₀ (38.37 nM) as α -MI (IC₅₀ = 12 nM) and α -GI (IC₅₀ = 20 nM). However, while α -MI and α -GI showed no effects on α 2 β 2, α 3 β 2, α 3 β 4, α 4 β 2, α 4 β 4 and α 7 receptors [32], GaIA remarkably exhibited also some potency at the α 9 α 10 (IC₅₀ = 777.2 nM), α 3 β 2 (IC₅₀ = 988.9 nM), the closely related α 6/ α 3 β 2 β 3 (IC₅₀ = 1170 nM, as well as the α 4 β 2

(IC₅₀ = 3931 nM), $\alpha 7$ (IC₅₀ = 5158 nM), $\alpha 2\beta 2$ (IC₅₀ = 6474 nM), and $\alpha 3\beta 4$ (IC₅₀ = 7912 nM) neuronal nAChRs.

Thus, AdIA and particularly GaIA display a wider pharmacological profile on nAChR subtypes compared to the other characterized members of this family and might provide a template for further structure–activity studies.

4. Materials and Methods

4.1. Abbreviations

Acm, acetamidomethyl; ACN, acetonitrile; DCM, dichloromethane; DMF, N,N-dimethylformamide; DIPC, diisopropylcarbodiimide; DTT, dithiothreitol; DTC, diethyldithiocarbamate; DSF, disulfiram; eq, equivalent; ESI-MS, electrospray ionization-mass spectrometry; FA, formic acid; Fmoc, fluorenylmethoxycarbonyl; GSH, reduced glutathione; GSSH, oxidized glutathione; IPA, isopropanol; LC/MS, liquid chromatography/mass spectrometry; nAChRs, nicotinic acetylcholine receptors; NBzl, 2-nitrobenzyl; RP-HPLC, reversed-phase high-performance liquid chromatography; SPPS, solid-phase peptide synthesis; TFA, trifluoroacetic acid; TIS, triisopropylsilane; Tris, 2-amino-2-(hydroxymethyl)propane-1,3-diol; Trt, trityl; UV, ultraviolet.

4.2. Chemical Synthesis

4.2.1. General Procedure for the Synthesis of Linear Conotoxin Peptides

The linear precursors of conotoxins were synthesized on a Liberty Blue peptide synthesis instrument (CEM, Matthews, NC, USA) at a scale of 0.1 mmol. The synthesis was conducted on a Rink-amide resin with a loading capacity of 0.34 mmol/g. The standard amino acid coupling cycle is as follows: 2.5 mL of amino acid (5 eq) are added to the reactor, activated with 1 mL of diisopropylcarbodiimide (DIPC) (5 equiv.) and 0.5 mL of Pure Oxyma (10 equiv.). The resulting mixture was heated at 90 °C in the microwave for 2.15 min. After each coupling reaction, the resin was subjected to a deprotection cycle of 2 min at 90 °C under microwave with a solution of DMF/Piperidine (80/20) followed by washing with DMF. Side-chain (except Acm and Nbzl) deprotection and cleavage from the resin were carried out using 10 mL of TFA/TIS/H₂O/DTT (88/2/5/5) (*v/v*) under agitation for 2 to 3 h. The reaction mixture was filtered, and the filtrate was dropwise added to cold diethyl ether to give a crude peptide precipitate and centrifuged. This synthetic method was applied to all synthetic conotoxin precursors, which were obtained with correct yields.

4.2.2. General Procedure for the Synthesis of Conotoxin via NBzl Protecting Group

The lyophilized linear conotoxin peptide was dissolved (0.5 mM) in 6 M Gn·HCl buffer, pH 7, and treated with 10 equiv. DSF for 10 s at 37 °C. Subsequently, the reaction mixture pH was adjusted to 6 using 0.1 M HCl and exposed to UV radiation at 350 nm (24 watts, ca. 3×10^{16} s cm⁻³ photons) in a photochemical 16 chamber reactor under ice-cooled conditions for 8–10 min. Purification was performed by using a semi-preparative C18 column.

4.2.3. General Procedure for the Synthesis of Conotoxin via Acm Protecting Group

The lyophilized linear conotoxin peptide (AdIA or GaIA) was dissolved (0.5 mM) in 6 M Gn·HCl buffer, pH 7, and treated with 10 equiv. DSF for 10 s at 37 °C. Subsequently, the reaction mixture pH was adjusted to 1 using 0.1 M HCl, treated with 10 equiv. PdCl₂, and incubated at 37.0 °C for 5 min. The reaction mixture was further treated with 30 equiv. of DTC (12 μ L) followed by 10 equiv. of DSF, and the pH of the reaction was adjusted to 6.0 using 0.1 M HCl to complete the reaction.

4.2.4. General Procedure for the Synthesis of Conotoxin via Oxidative Folding

The lyophilized linear conotoxin peptide (0.25 mM) was dissolved in the selected buffer solution and subjected to agitation for 48 h. Upon completion of the reaction, the mixture was acidified to pH 3 using a 10% formic acid solution for subsequent analyses.

Based on Gyanda et al. [28], the samples underwent UHPLC-HRMS analysis, and the peak areas were measured after ion extraction of the compound to determine the proportion of each isomer generated during the oxidative folding process.

4.3. Mass Spectrometry

Analytical HPLC was performed on a Dionex Ultimate 3000 (Thermo Fisher Scientific, Waltham, MA, USA), using analytical XBridge Peptide BEH C₁₈, 3.5 µm, Column (4.6 × 150 mm, 300 Å) (Waters Corporation, Milford, MA, USA) at a flow rate of 1.2 mL/min, coupled with a diode array. All solvents used were HPLC-grade.

The LC-MS system consists of a Thermo Fisher Scientific LC-MS device, an Accela HPLC coupled to a QFleet fitted with an electrospray ionization source, and an ion-trap analyzer. All analyses were performed using a Kinetex 2.6 µm C₁₈ column (150 × 3.00 mm) from Phenomenex Inc. (Torrance, CA, USA) in linear gradient mode from 2% to 60% over 30 min with a flow rate of 0.5 mL/min (solvent A, water + 0.1% FA; solvent B, acetonitrile + 0.1% FA).

The UHPLC/HRMS system consists of a Vanquish UHPLC (Thermo Fisher Scientific, Waltham, MA, USA) coupled to a QTOF Maxis II mass spectrometer (Bruker Daltonics, Billerica, MA, USA), source electrospray ionization mode, ESI+. All analyses were performed using a bioZen™ 2.6 µm Peptide XB-C₁₈ column (150 × 2.1 mm, 100 Å) (Phenomenex, Torrance, CA, USA) in linear gradient mode from 2% to 50% over 50 min with a flow rate of 0.3 mL/min (solvent A, water + 0.1% FA; solvent B, acetonitrile + 0.1% FA) at 40 °C. Acetonitrile and formic acid RS for LC-MS (Carlo Erba, Val de Reuil, France); ultra-pure water from PURELAB Chorus 1 (ELGA Veolia, Lane End, UK).

4.4. Preparative RP-HPLC

Semi-preparative purification of cyclic peptides was performed using a Waters 1525 chromatography system fitted with a Waters 2487 tunable absorbance detector with detection at 214 nm and 254 nm. Purification was performed by eluting buffer A (H₂O, 0.1% FA) into buffer B (acetonitrile + 0.1% FA). The column used was a GRACE Vydac C-18 column (250 × 10 mm, 5 µm) (Thermo Fisher Scientific, Waltham, MA, USA) at a flow rate of 3 mL/min.

4.5. Electrophysiology

Plasmids encoding the neuronal nAChR subunits (rat α₂, α₃, α₄, α₆, β₂, β₃, β₄) were provided by Jim Patrick (Baylor College of Medicine, Houston, TX, USA) and subcloned in pNKS2. Rat muscle α₁, β₁, γ, and δ subunits in pSPOoD were provided by Veit Witzemann (MPI for Medical Research, Heidelberg, Germany). The α₆/α₃ chimera was generated in pNKS according to [35–37]. Rat α₉ and α₁₀ nAChR subunits in pBS KS(-) were provided by B. Elgoyhen and J. Boulter (The Salk Institut; San Diego, UCLA Department of Psychiatry and Biobehavioral Sciences, California) and were subcloned in pNKS2. The subunit ratio of α₉/α₁₀ was 3:1. Oocytes were obtained from EcoCyte Bioscience (Dortmund, Germany) or surgically extracted (Az. 2532.Vet_03-19-77) from female *Xenopus laevis* (Nasco, Fort Atkinson, WI, USA) and kept at the core facility animal models of the biomedical center of the LMU Munich (Az:4.3.2-5682/LMU/BMC/CAM) in accordance with the EU Animal Welfare Act.

Functional experiments were performed as previously described by Giribaldi et al. [35]. Briefly, plasmids were linearized and cRNA synthesized using the mMessageMachine kit (Invitrogen, Thermo Fisher Scientific, Waltham, MA, USA). Fifty nanoliters of cRNA (0.1–0.5 µg/µL) were injected per oocyte with equal ratios of subunits. Oocytes were stored at 16 °C in sterile filtered ND96 (96 mM NaCl, 2 mM KCl, 1 mM CaCl₂, 1 mM MgCl₂, 5 mM HEPES, and pH 7.4) containing 5 µg/mL gentamicin. After 1–4 days, two-electrode voltage clamp recordings were performed at –70 mV with a Turbo Tec 05X Amplifier (npi electronic, Tamm, Germany) and CellWorks software (version 6.2.2). Electrode resistances were less than 1 MΩ, and currents were filtered at 200 Hz and digitized at 400 Hz. The

recording solution ND96, with or without 100 μ M ACh, was automatically applied via a custom-made magnetic valve system combined with a manifold mounted closely above the oocyte, thus allowing a fast (<300 ms) and reproducible solution exchange. Agonist pulses (2 s) were applied in 4-min intervals. Toxins were manually applied from a 10 \times stock solution in the 50- μ L measuring chamber and preincubated for 3 min. Current responses were normalized to control responses before toxin application. GraphPad Prism (version 9.3.1) was used for data analysis, and a four-parameter logistic fit (Hill-fit) with plateaus constrained to 100% and 0% was used to generate dose–response curves. Oocytes from at least two frogs were used for each data point.

Supplementary Materials: The following supporting information can be downloaded at: <https://www.mdpi.com/article/10.3390/md21060356/s1>, Table S1: Amino acid sequence of linear conotoxin peptides synthesized; Figure S1: One pot regioselective oxidation of GaIA; Figure S2: LC–MS analysis one-pot regioselective oxidation of AdIA; Figure S3: Temperature-dependent HPLC; analyses of AdIA cis/trans conformations; Figure S4: UHPLC-HRMS analysis of synthetic folded GaIA; Figure S5: UHPLC-HRMS analysis of synthetic folded AdIA; Figure S6: UHPLC-HRMS analysis of synthetic ribbon and globular AdIA; Figure S7: Various oxidative folding conditions tested on GaIA; Figure S8: Various oxidative folding conditions tested on AdIA; Figure S9: Comparison of oxidative folding and regioselective folding on AdIA.

Author Contributions: Conceptualization, Y.M.S., S.D. and N.I.; methodology, Y.M.S., V.K., G.L. and Y.S.; validation, A.B., A.N., S.D. and N.I.; formal analysis and data curation, Y.M.S., V.K., D.R. and G.L.; writing—original draft preparation, Y.M.S.; writing—review and editing, S.D., A.N. and N.I.; supervision, S.D. and N.I. All authors have read and agreed to the published version of the manuscript.

Funding: This research was funded by a Ph.D. scholarship from the UPVD and Polycone ANR-20-BFOC-0005 to YMS, and the Deutsche Forschungsgemeinschaft (DFG, German Research Foundation, Research Training Group GRK2338, P01, to A.N.).

Data Availability Statement: Not applicable.

Acknowledgments: We thank Guy Kamnesky (Schulich Faculty of Chemistry, Technion, Israel) for his valuable support and advice on peptide synthesis and Jules Kotarba (CRIOBE, University of Perpignan Via Domitia, France) for supplying the chemical materials. We thank the Departmental Council of Mayotte (CDM) for the scholarship to YMS and the French Group of Peptides and Proteins (GFPP) for funding the internship at the Brick’s group in Israel, as well as the Languedoc Roussillon Doctoral College (CDLR) and Doctoral School 305 (ED305). We thank the government of French Polynesia for providing us with the cone snail resources and the authorizations to carry out our research.

Conflicts of Interest: The authors declare no conflict of interest.

References

1. Georges, R.; Michael, R. *PANORAMA SUR LA DIVERSITE DES CONIDAE 110 Espèces Prédatrices Des plus Efficaces*; Association Française de Conchyliologie: Paris, France, 2021; p. 162.
2. Kaas, Q.; Westermann, J.-C.; Craik, D.J. Conopeptide Characterization and Classifications: An Analysis Using ConoServer. *Toxicon* **2010**, *55*, 1491–1509. [[CrossRef](#)] [[PubMed](#)]
3. Miljanich, G.P. Ziconotide: Neuronal Calcium Channel Blocker for Treating Severe Chronic Pain. *Curr. Med. Chem.* **2004**, *11*, 3029–3040. [[CrossRef](#)] [[PubMed](#)]
4. Dani, J.A.; Bertrand, D. Nicotinic Acetylcholine Receptors and Nicotinic Cholinergic Mechanisms of the Central Nervous System. *Annu. Rev. Pharmacol. Toxicol.* **2007**, *47*, 699–729. [[CrossRef](#)] [[PubMed](#)]
5. Hone, A.J.; McIntosh, J.M. Nicotinic Acetylcholine Receptors in Neuropathic and Inflammatory Pain. *FEBS Lett.* **2018**, *592*, 1045–1062. [[CrossRef](#)]
6. Hone, A.J.; McIntosh, J.M. Nicotinic Acetylcholine Receptors: Therapeutic Targets for Novel Ligands to Treat Pain and Inflammation. *Pharmacol. Res.* **2023**, *190*, 106715. [[CrossRef](#)]
7. Papke, R.L.; Lindstrom, J.M. Nicotinic Acetylcholine Receptors: Conventional and Unconventional Ligands and Signaling. *Neuropharmacology* **2020**, *168*, 108021. [[CrossRef](#)]
8. Albuquerque, E.X.; Pereira, E.F.R.; Alkondon, M.; Rogers, S.W. Mammalian Nicotinic Acetylcholine Receptors: From Structure to Function. *Physiol. Rev.* **2009**, *89*, 73–120. [[CrossRef](#)]

9. Kalamida, D.; Poulas, K.; Avramopoulou, V.; Fostieri, E.; Lagoumintzis, G.; Lazaridis, K.; Sideri, A.; Zouridakis, M.; Tzartos, S.J. Muscle and Neuronal Nicotinic Acetylcholine Receptors. *FEBS J.* **2007**, *274*, 3799–3845. [[CrossRef](#)]
10. Giribaldi, J.; Dutertre, S. α -Conotoxins to Explore the Molecular, Physiological and Pathophysiological Functions of Neuronal Nicotinic Acetylcholine Receptors. *Neurosci. Lett.* **2018**, *679*, 24–34. [[CrossRef](#)]
11. Dutertre, S.; Nicke, A.; Tsetlin, V.I. Nicotinic Acetylcholine Receptor Inhibitors Derived from Snake and Snail Venoms. *Neuropharmacology* **2017**, *127*, 196–223. [[CrossRef](#)]
12. Dani, J.A. Neuronal Nicotinic Acetylcholine Receptor Structure and Function and Response to Nicotine. *Int. Rev. Neurobiol.* **2015**, *124*, 3–19. [[CrossRef](#)]
13. Azam, L.; Dowell, C.; Watkins, M.; Stitzel, J.A.; Olivera, B.M.; McIntosh, J.M. α -Conotoxin BuIA, a Novel Peptide from *Conus Bullatus*, Distinguishes among Neuronal Nicotinic Acetylcholine Receptors. *J. Biol. Chem.* **2005**, *280*, 80–87. [[CrossRef](#)]
14. Zhu, X.; Wang, S.; Kaas, Q.; Yu, J.; Wu, Y.; Harvey, P.J.; Zhangsun, D.; Craik, D.J.; Luo, S. Discovery, Characterization, and Engineering of LvIC, an A4/4-Conotoxin That Selectively Blocks Rat A6/A3 β 4 Nicotinic Acetylcholine Receptors. *J. Med. Chem.* **2023**, *66*, 2020–2031. [[CrossRef](#)]
15. Wei, N.; Chu, Y.; Liu, H.; Xu, Q.; Jiang, T.; Yu, R. Antagonistic Mechanism of α -Conotoxin BuIA toward the Human A3 β 2 Nicotinic Acetylcholine Receptor. *ACS Chem. Neurosci.* **2021**, *12*, 4535–4545. [[CrossRef](#)]
16. Ning, J.; Li, R.; Ren, J.; Zhangsun, D.; Zhu, X.; Wu, Y.; Luo, S. Alanine-Scanning Mutagenesis of α -Conotoxin GI Reveals the Residues Crucial for Activity at the Muscle Acetylcholine Receptor. *Mar. Drugs* **2018**, *16*, 507. [[CrossRef](#)]
17. Kapon, C.A.; Thapa, P.; Cabaltea, C.C.; Guendisch, D.; Collier, A.C.; Bingham, J.-P. Conotoxin Truncation as a Post-Translational Modification to Increase the Pharmacological Diversity within the Milked Venom of *Conus Magus*. *Toxicon* **2013**, *70*, 170–178. [[CrossRef](#)]
18. Cruz, L.J.; Gray, W.R.; Olivera, B.M.; Zeikus, R.D.; Kerr, L.; Yoshikami, D.; Moczydlowski, E. *Conus Geographus* Toxins That Discriminate between Neuronal and Muscle Sodium Channels. *J. Biol. Chem.* **1985**, *260*, 9280–9288. [[CrossRef](#)]
19. Chi, S.-W.; Kim, D.-H.; Olivera, B.M.; McIntosh, J.M.; Han, K.-H. NMR Structure Determination of α -Conotoxin BuIA, a Novel Neuronal Nicotinic Acetylcholine Receptor Antagonist with an Unusual 4/4 Disulfide Scaffold. *Biochem. Biophys. Res. Commun.* **2006**, *349*, 1228–1234. [[CrossRef](#)] [[PubMed](#)]
20. Laps, S.; Sun, H.; Kamnesky, G.; Brik, A. Palladium-Mediated Direct Disulfide Bond Formation in Proteins Containing S-Acetamidomethyl-Cysteine under Aqueous Conditions. *Angew. Chem. Int. Ed.* **2019**, *58*, 5729–5733. [[CrossRef](#)] [[PubMed](#)]
21. Laps, S.; Atamleh, F.; Kamnesky, G.; Sun, H.; Brik, A. General Synthetic Strategy for Regioselective Ultrafast Formation of Disulfide Bonds in Peptides and Proteins. *Nat. Commun.* **2021**, *12*, 870. [[CrossRef](#)] [[PubMed](#)]
22. Jin, A.-H.; Brandstaetter, H.; Nevin, S.T.; Tan, C.C.; Clark, R.J.; Adams, D.J.; Alewood, P.F.; Craik, D.J.; Daly, N.L. Structure of α -Conotoxin BuIA: Influences of Disulfide Connectivity on Structural Dynamics. *BMC Struct. Biol.* **2007**, *7*, 28. [[CrossRef](#)]
23. Kuryatov, A.; Berrettini, W.; Lindstrom, J. Acetylcholine Receptor (AChR) A5 Subunit Variant Associated with Risk for Nicotine Dependence and Lung Cancer Reduces (A4 β 2) α 5 AChR Function. *Mol. Pharmacol.* **2011**, *79*, 119–125. [[CrossRef](#)]
24. Dutertre, S.; Jin, A.-H.; Vetter, I.; Hamilton, B.; Sunagar, K.; Lavergne, V.; Dutertre, V.; Fry, B.G.; Antunes, A.; Venter, D.J.; et al. Evolution of Separate Predation- and Defence-Evoked Venoms in Carnivorous Cone Snails. *Nat. Commun.* **2014**, *5*, 3521. [[CrossRef](#)] [[PubMed](#)]
25. Jin, A.-H.; Muttenthaler, M.; Dutertre, S.; Himaya, S.W.A.; Kaas, Q.; Craik, D.J.; Lewis, R.J.; Alewood, P.F. Conotoxins: Chemistry and Biology. *Chem. Rev.* **2019**, *119*, 11510–11549. [[CrossRef](#)]
26. Kaas, Q.; Yu, R.; Jin, A.-H.; Dutertre, S.; Craik, D.J. ConoServer: Updated Content, Knowledge, and Discovery Tools in the Conopeptide Database. *Nucleic Acids Res.* **2012**, *40*, D325–D330. [[CrossRef](#)] [[PubMed](#)]
27. Morrison, K.L.; Weiss, G.A. Combinatorial Alanine-Scanning. *Curr. Opin. Chem. Biol.* **2001**, *5*, 302–307. [[CrossRef](#)]
28. Gyanda, R.; Banerjee, J.; Chang, Y.-P.; Phillips, A.M.; Toll, L.; Armishaw, C.J. Oxidative Folding and Preparation of α -Conotoxins for Use in High-Throughput Structure–Activity Relationship Studies. *J. Pept. Sci.* **2013**, *19*, 16–24. [[CrossRef](#)]
29. Wu, X.; Wu, Y.; Zhu, F.; Yang, Q.; Wu, Q.; Zhangsun, D.; Luo, S. Optimal Cleavage and Oxidative Folding of α -Conotoxin TxIB as a Therapeutic Candidate Peptide. *Mar. Drugs* **2013**, *11*, 3537–3553. [[CrossRef](#)] [[PubMed](#)]
30. Postma, T.M.; Albericio, F. Disulfide Formation Strategies in Peptide Synthesis: Disulfide Formation Strategies in Peptide Synthesis. *Eur. J. Org. Chem.* **2014**, *2014*, 3519–3530. [[CrossRef](#)]
31. Góngora-Benítez, M.; Tulla-Puche, J.; Albericio, F. Multifaceted Roles of Disulfide Bonds. Peptides as Therapeutics. *Chem. Rev.* **2014**, *114*, 901–926. [[CrossRef](#)]
32. Postma, T.M.; Albericio, F. *N*-Chlorosuccinimide, an Efficient Reagent for On-Resin Disulfide Formation in Solid-Phase Peptide Synthesis. *Org. Lett.* **2013**, *15*, 616–619. [[CrossRef](#)] [[PubMed](#)]
33. Spears, R.J.; McMahon, C.; Chudasama, V. Cysteine Protecting Groups: Applications in Peptide and Protein Science. *Chem. Soc. Rev.* **2021**, *50*, 11098–11155. [[CrossRef](#)] [[PubMed](#)]
34. Azam, L.; Maskos, U.; Changeux, J.-P.; Dowell, C.D.; Christensen, S.; De Biasi, M.; McIntosh, J.M. α -Conotoxin BuIA[T5A;P6O]: A Novel Ligand That Discriminates between A6 β 4 and A6 β 2 Nicotinic Acetylcholine Receptors and Blocks Nicotine-Stimulated Norepinephrine Release. *FASEB J. Off. Publ. Fed. Am. Soc. Exp. Biol.* **2010**, *24*, 5113–5123. [[CrossRef](#)] [[PubMed](#)]
35. Giribaldi, J.; Wilson, D.; Nicke, A.; El Hamdaoui, Y.; Laconde, G.; Faucherre, A.; Moha Ou Maati, H.; Daly, N.L.; Enjalbal, C.; Dutertre, S. Synthesis, Structure and Biological Activity of CIA and CIB, Two α -Conotoxins from the Predation-Evoked Venom of *Conus Catus*. *Toxins* **2018**, *10*, 222. [[CrossRef](#)] [[PubMed](#)]

36. McIntosh, J.M.; Azam, L.; Staheli, S.; Dowell, C.; Lindstrom, J.M.; Kuryatov, A.; Garrett, J.E.; Marks, M.J.; Whiteaker, P. Analogs of Alpha-Conotoxin MII Are Selective for Alpha6-Containing Nicotinic Acetylcholine Receptors. *Mol. Pharmacol.* **2004**, *65*, 944–952. [[CrossRef](#)] [[PubMed](#)]
37. Kuryatov, A.; Olale, F.; Cooper, J.; Choi, C.; Lindstrom, J. Human A6 AChR Subtypes: Subunit Composition, Assembly, and Pharmacological Responses. *Neuropharmacology* **2000**, *39*, 2570–2590. [[CrossRef](#)]

Disclaimer/Publisher’s Note: The statements, opinions and data contained in all publications are solely those of the individual author(s) and contributor(s) and not of MDPI and/or the editor(s). MDPI and/or the editor(s) disclaim responsibility for any injury to people or property resulting from any ideas, methods, instructions or products referred to in the content.